Gas flow observer for Diesel Engines with EGR

Master's thesis
performed in **Vehicular Systems**

by
Fredrik Swartling

Reg nr: LiTH-ISY-EX-3692-2005

15th June 2005

Gas flow observer for Diesel Engines with EGR

Master's thesis

performed in **Vehicular Systems**,
Dept. of Electrical Engineering
at **Linköpings universitet**

by **Fredrik Swartling**

Reg nr: LiTH-ISY-EX-3692-2005

Supervisor: **Mattias Nyberg**
Scania CV AB
Jesper Ritzén
Scania CV AB

Examiner: **Assistant Professor Erik Frisk**
Linköpings Universitet

Linköping, 15th June 2005

Avdelning, Institution Division, Department Vehicular Systems, Dept. of Electrical Engineering 581 83 Linköping	**Datum** Date 15th June 2005

Språk Language ☐ Svenska/Swedish ☒ Engelska/English ☐ ________________	**Rapporttyp** Report category ☐ Licentiatavhandling ☒ Examensarbete ☐ C-uppsats ☐ D-uppsats ☐ Övrig rapport ☐ ________________	**ISBN** — **ISRN** LITH-ISY-EX-3692-2005 **Serietitel och serienummer** Title of series, numbering **ISSN** —

URL för elektronisk version

http://www.vehicular.isy.liu.se
http://www.ep.liu.se/exjobb/isy/2005/3692/

Titel Gasflödesobservatör för dieselmotorer med EGR

Title Gas flow observer for Diesel Engines with EGR

Författare
Author
Fredrik Swartling

Sammanfattning
Abstract

Due to stricter emission legislation, there is a need for more efficient control of diesel engines with exhaust gas recirculation(EGR). In particular, it is important to estimate the air/fuel ratio accurately in transients. Therefore a new engine gas flow model has been developed. This model divides the gas into one part for oxygen and one part for inert gases. Based on this model an observer has been designed to estimate the oxygen concentration in the gas going into the engine, which can be used to calculate the air/fuel ratio. This observer can also be used to estimate the intake manifold pressure. The advantage of estimating the pressure, instead of low pass filtering the noisy signal, is that the observer does not cause time delay.

Nyckelord
Keywords
EGR, Mean Value Engine Model, Observer, Lambda

Abstract

Due to stricter emission legislation, there is a need for more efficient control of diesel engines with exhaust gas recirculation(EGR). In particular, it is important to estimate the air/fuel ratio accurately in transients. Therefore a new engine gas flow model has been developed. This model divides the gas into one part for oxygen and one part for inert gases. Based on this model an observer has been designed to estimate the oxygen concentration in the gas going into the engine, which can be used to calculate the air/fuel ratio. This observer can also be used to estimate the intake manifold pressure. The advantage of estimating the pressure, instead of low pass filtering the noisy signal, is that the observer does not cause time delay.

Keywords: EGR, Mean Value Engine Model, Observer, Lambda

Preface

This master's thesis has been performed for Scania CV AB at the division of Engine Software and OBD (NEE) during the spring of 2005.

Thesis outline

Chapter 1 A short introduction to the background and the objectives of this thesis

Chapter 2 The basics of combustion chemistry

Chapter 3 The model on which the observer is based is described

Chapter 4 The observer design

Chapter 5 Measurements that were done in the EGR system

Chapter 6 Conclusions and future work

Acknowledgment

I would like to thank my supervisors at Scania, Jesper Ritzén and Mattias Nyberg and my examiner Erik Frisk for many inspiring discussions and your support. Thanks also to all the helpful people at Scania, in particular David Elfvik and Mats Jennische at for always taking your time to help me and answer my questions about engine control.

Fredrik Swartling
Södertälje, June 2005

Contents

Abstract **v**

Preface and Acknowledgment **vi**

1 Introduction **1**
1.1 Background 1
1.2 Objectives 2
1.3 Methods 2

2 Combustion Chemistry **3**
2.1 Stoichiometric Combustion 3
2.2 Definition of λ_{true} 4
2.3 Derivation and definition of λ_{O_2} 4

3 Engine modeling **7**
3.1 Introduction 7
3.2 Choice of model states 8
3.3 Model structure 9
3.3.1 Compressor 9
3.3.2 Intake Manifold 9
3.3.3 Combustion 10
3.3.4 Exhaust Manifold 11
3.3.5 EGR 11
3.3.6 Turbine 12
3.3.7 Exhaust System 12
3.3.8 Turbocharger 13

4 Observer design **15**
4.1 Properties of the Observed System 15
4.2 Design Method 17
4.3 Calculating Noise Matrices 18
4.3.1 Calculating R 19
4.3.2 Calculating Q 20

4.4 Observer designs comparisons 23
4.4.1 Evaluating the need for multiple linearizations . . . 23
4.4.2 Evaluating the possibility to calculate K off-line . . . 24
4.5 Evaluation 24
4.5.1 Comparison with low pass filtering 24
4.5.2 Evaluation of λ observer 27

5 Validation of EGR flow **29**
5.1 Introduction 29
5.2 The Catalytic Converter Experiment 29
5.2.1 Theoretical Background 29
5.2.2 Experimental Setup 30
5.2.3 Results 30
5.3 Conclusion 31

6 Conclusions and Future Work **33**
6.1 Conclusions 33
6.2 Future work 33

References **35**

Notation **37**

A Derivation of λ_{true} **39**

Chapter 1

Introduction

1.1 Background

Due to stricter emission legislation for heavy duty trucks, manufacturers have come up with new methods to reduce emissions. One popular method is exhaust gas recirculation(EGR).

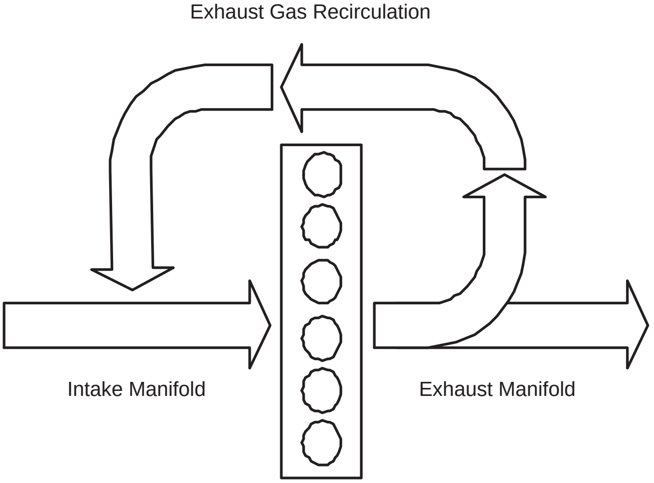

Figure 1.1: Overview of EGR system

The basic idea with exhaust gas recirculation is to lead some of the exhaust gas back into the engine, as shown in Figure 1.1. This lowers the combustion temperature and leads to reduced NOx emissions since NOx production is closely related to the peak temperature of the combustion. The combustion temperature will be lowered because the recirculated exhaust gas has a reduced concentration of oxygen and increased concentration of inert gases, i.e. gases that do not participate in the combustion. Even though the inert gases do not participate in the combustion they absorb released energy, and this reduces the combustion temperature.

To be able to model the NOx production and control the engine, estimating the oxygen concentration in the gas flow is important. Today there is a good knowledge of the gas flow in an EGR engine during steady state, and this has been enough to be able to control the engine to meet the EURO4 legislation that came into place in 2005. However for the EURO5 legislation that will come into place 2008, knowing the properties of the system during transients will be essential.

1.2 Objectives

The objective of this thesis is to examine the possibilities of designing an observer that will be able to do the following:

- Estimate the flow of pure air into the engine
- Estimate the oxygen concentration in the flow into the engine
- Estimate the EGR flow
- Filter noise from measurable signals without unnecessary time delay

Improved measurement of flow of pure air is needed to improve the fuel injection control during transients. The oxygen concentration can be used as input to a NOx model. Knowing the EGR flow is important when controlling the EGR valve and the variable geometry turbocharger(VGT).

1.3 Methods

In the first stage of the thesis an existing model described by Elfvik [5], Ritzén [6] and Ericsson [7] will be modified to suit the objectives of the thesis. Using this model a observer will be designed and implemented in Simulink. Together with measurement data from a 6 cylinder Scania engine, the performance of the observer will be evaluated.

Chapter 2

Combustion Chemistry

When deciding how much fuel to inject in the engine it is important to know how much air there is available. This chapter is a short resume of the chemistry of the combustion, old ways of keeping track of the air/fuel ratio, and in the end a proposal of how the air/fuel ratio could be defined in a way that suits EGR engines better.

2.1 Stoichiometric Combustion

During internal combustion, fuel is burnt in the presence of the oxygen in the air, resulting in water and carbon dioxide as shown in Eq. 2.1[1].

$$C_aH_b + \left(a + \frac{b}{4}\right)(O_2 + 3.773N_2) \longrightarrow aCO_2 + \frac{b}{2}H_2O + 3.773\left(a + \frac{b}{4}\right)N_2 \tag{2.1}$$

The parameters a and b represent the number of carbon and hydrogen atoms in one molecule of fuel. More interesting than the exact dimension of a and b is the relation between them, $y = \frac{b}{a}$, which shows the relative amount of carbon in the fuel. To balance Eq. 2.1, the amount of fuel and air going in to the reaction has to be in balance. Here air is supposed to have the composition $(O_2 + 3.773N_2)$. When this balance between the fuel mass and the air mass is achieved, the air/fuel proportion is stoichiometric. The stoichiometric relation of fuel and air in Eq. 2.1 is derived in Eq. 2.2.

$$\left(\frac{A}{F}\right)_s = \frac{(1 + \frac{y}{4})(m_{O_2} + 3.773m_{N_2})}{m_C + m_H y} \tag{2.2}$$

where m_{O_2},m_{N_2},m_C and m_H are molecule masses. Normally $\left(\frac{A}{F}\right)_s$ is around 14.7, i.e. the mass of the air has to be 14.7 times larger than the mass of the fuel for the reaction to be balanced.

$$\lambda_{meas} = \frac{\dot{m}_{air}}{\dot{m}_{fuel}\left(\frac{A}{F}\right)_s} \tag{2.3}$$

λ, defined in Eq. 2.3, is a measurement of the composure of air and fuel relative the stoichiometric proportion. $\lambda = 1$ corresponds to a stoichiometric composure and $\lambda > 1$ indicates a surplus of air. A diesel engine is always run with $\lambda > 1.3$ to avoid smoke. The name, λ_{meas}, comes from the fact that this λ can be measured with a λ-sensor that is put in the exhaust manifold. The sensor measures the oxygen concentration in the exhaust gas and estimates the surplus or lack of air going into the engine, taking the oxygen concentration in air as a constant.

2.2 Definition of λ_{true}

λ_{meas} is the relation between the air coming from the compressor and the fuel. What is interesting in reality is the ratio between the total flow of air from the compressor plus the air from EGR and the fuel. This is referred to as λ_{true}. For steady state it is possible to derive a simple relation between λ_{true} and λ_{meas} using the ratio between the EGR flow and the total flow, $EGR\%$. Eq. 2.4 shows this relationship and all the derivations are showed in appendix A. This is a relation used today for engine control.

$$\lambda_{true} = \frac{\lambda_{meas} - EGR\%}{1 - EGR\%} \tag{2.4}$$

$$EGR\% = \frac{\dot{m}_{egr}}{\dot{m}_{eng,in,tot}} \tag{2.5}$$

2.3 Derivation and definition of λ_{O_2}

λ_{true} gives a good value in steady state, but in transients some of the assumptions made in the derivation of Eq. 2.4 are not valid. A way to work around this problem is to make a model like the one in Figure 2.1. By continually keeping track of the oxygen concentration, λ can be defined as

$$\lambda_{O_2} = \frac{\dot{m}_{im,O_2}}{\dot{m}_{fuel}\left(\frac{O}{F}\right)_s} \tag{2.6}$$

where $\left(\frac{O}{F}\right)_s$ is the stoichiometric relation between oxygen and fuel. $\dot{m}_{im,O_2}$ is the oxygen part of the flow into the engine.

$$\left(\frac{O}{F}\right)_s = \frac{(1+\frac{y}{4})m_{O_2}}{m_C + m_H y} \tag{2.7}$$

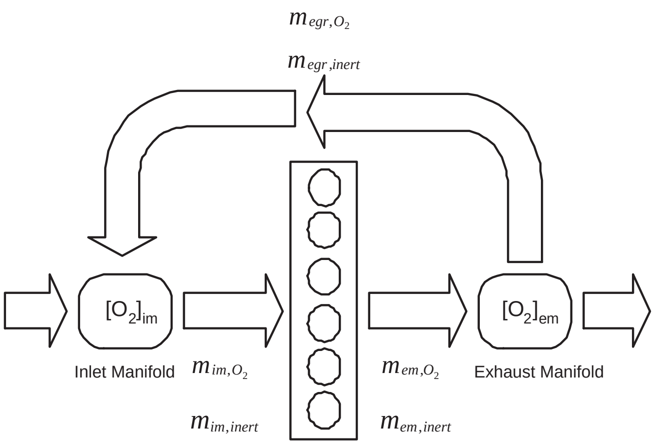
m_{egr,O_2}
$m_{egr,inert}$
$[O_2]_{im}$
$[O_2]_{em}$
Inlet Manifold
m_{im,O_2}
m_{em,O_2}
Exhaust Manifold
$m_{im,inert}$
$m_{em,inert}$

Figure 2.1: Oxygen concentration state model

Using oxygen instead of air as the magnitude from where to calculate λ is a way to move away from the use of air as a unit and to make the calculations more intuitive. To know $\dot{m}_{im,O_2}$, a more elaborate model than the one used today is needed. The model has to be able to keep track of the oxygen concentration in the gas flows.

Chapter 3

Engine modeling

3.1 Introduction

In this chapter the model that will be used for the observer design will be described. The model is an extended version of a gas flow model developed in [5], [6] and [7]. Figure 3.1 and Table 3.1 show a model overview and explain the model's input signals.

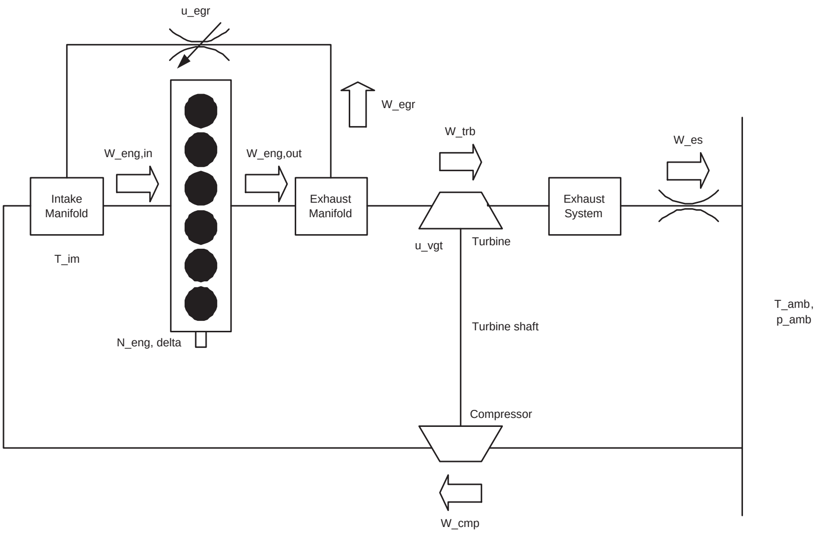
u_egr
W_egr
W_trb
W_es
W_eng,in
W_eng,out
Intake Manifold
Exhaust Manifold
Exhaust System
u_vgt
Turbine
T_im
T_amb,
p_amb
Turbine shaft
N_eng, delta
Compressor
W_cmp

Figure 3.1: Model with inputs and mass flows

Table 3.1: Explanations of input signals

Symbol	Description	Unit
N_{eng}	Engine speed	[rpm]
δ	Injected fuel	[kg/stroke]
T_{im}	Intake manifold temperature	[K]
p_{amb}	Ambient pressure	[Pa]
T_{amb}	Ambient temperature	[K]
u_{egr}	EGR valve position	[V]
u_{vgt}	VGT vane position	[V]

3.2 Choice of model states

One purpose with of the observer is to estimate the oxygen concentration in the gas that flows into the engine. To be able to know this it is necessary to know the oxygen concentration in all the gas flows around the engine. Therefore the original model has to be modified so that instead of having one gas flow between each control volume, there will be two gas flows. One flow for oxygen and one flow for inert gases. To be able to calculate two mass flows from each control volume, the volumes themself have to have two states containing information about the gas composition.

When selecting the states, there are two main choices to do. The first one is whether to use the pressure or the mass as the quantity for the amount of gas in a volume. The other one is whether to use oxygen concentration as a state or having two mass/pressure states for every control volume, one for oxygen and one for inert gases. After simulating and evaluating the model with different composition of states, two pressure states per volume was considered to be the best choice. The reasons for choosing partial pressure are listed below:

- More robust initial conditions
- Less calculations
- Simple relations to measurable quantities

The robustness of the initial conditions is due to the fact that the initial pressure is not linked to the size of the volume, which is the case when using mass states. One gets less calculations since the pressure has to be calculated even if the masses are used as states, because most gas flow formulas contain some kind of pressure relation. Also the simple relationship between the partial pressures and the measured static pressures makes the observer design simpler. Table 3.2 contains a summary of the selected model states. Notice that the exhaust pressure has not been divided into two states since the oxygen concentration in the exhaust system does not affect the engine.

Table 3.2: Model states

Symbol	Description	Unit
$p_{im,O2}$	Intake manifold oxygen pressure	[Pa]
$p_{im,inert}$	Intake manifold inert gas pressure	[Pa]
$p_{em,O2}$	Exhaust manifold oxygen pressure	[Pa]
$p_{em,inert}$	Exhaust manifold inert gas pressure	[Pa]
p_{es}	Exhaust system pressure	[Pa]
n_{trb}	Turbine speed	[rpm]

3.3 Model structure

In this section all the parts of the engine model are described. The order of the parts follows the air through the engine, and ends with the turbocharger.

3.3.1 Compressor

The compressor flow is modeled from a map, Eq. 3.1, and depends on the pressure ratio between p_{im} and p_{amb} and the turbine speed, n_{trb}.

$$W_{cmp,tot} = f_{W_{cmp}}\left(\frac{p_{im}}{p_{amb}}, n_{trb}\right) \tag{3.1}$$

The flow can be divided into an oxygen and an inert part as in Eq. 3.2 and 3.3 since the composition of pure air is well known. The mass of the oxygen is 23% of the total air mass.

$$W_{cmp,O2} = 0.23W_{cmp,tot} \tag{3.2}$$

$$W_{cmp,inert} = 0.77W_{cmp,tot} \tag{3.3}$$

3.3.2 Intake Manifold

The state equation for the pressure in all control volumes are derived from the ideal gas law. In Eq. 3.4 it is assumed that all pressure changes come from the changes in mass, not in temperature.

$$\dot{p} = \frac{RT}{V}\dot{m} = \frac{\widetilde{R}T}{MV}\dot{m} \tag{3.4}$$

where $\widetilde{R}$ is the universal gas constant, M the molecular weight and R is a gas specific constant that depends on mass of the molecules. Applying Eq. 3.4 to the intake manifold gives the following equations for $\dot{p}_{im,O2}$ and $\dot{p}_{im,inert}$:

$$\dot{p}_{im,O2} = \frac{R_{O2}T_{im}}{V_{im}}\left(W_{cmp,O2} + W_{egr,O2} - W_{eng,in,O2}\right) \tag{3.5}$$

$$\dot{p}_{im,inert} = \frac{R_{inert}T_{im}}{V_{im}}\left(W_{cmp,inert} + W_{egr,inert} - W_{eng,in,inert}\right) \quad (3.6)$$

where

$$p_{im,tot} = p_{im,inert} + p_{im,O2} \quad (3.7)$$

3.3.3 Combustion

The volume flow of air into the engine is $\frac{V_d N_{eng}}{120}$. To get the mass flow into the engine, the volume flow is combined with p_{im},R_{im},T_{im} and the ideal gas law. This gives the ideal flow into the engine, but in reality this is not possible to achieve. Depending on p_{im}, R_{im}, T_{im} and N_{eng} this will be more or less achievable. To compensate for this the ideal flow is multiplied with the volumetric efficiency, η_{vol}, in Eq. 3.8 to give the total flow into the engine.

$$W_{eng,in,tot} = \eta_{vol}\frac{V_d N_{eng} p_{im}}{120 R_{im} T_{im}} \quad (3.8)$$

η_{vol} is mapped from measurement data with axes as in Eq. 3.9.

$$\eta_{vol} = f_{\eta_{vol}}\left(N_{eng}, \frac{p_{im}}{T_{im}R_{im}}\right) \quad (3.9)$$

Having the total flow into the engine and the gas composition in the intake manifold, it is now possible to derive an expression for the composition of the gas that flows into the engine. The assumption that is made is that the flow out of a volume has the same composition as the gas in the volume. W_{O2} can then be derived from p_{O2}, p_{inert} and $\dot{m}_{tot}$ as follows.

$$W_{O2} = \frac{m_{O2}}{m_{tot}}\dot{m}_{tot} = \frac{\frac{p_{O2}V}{R_{O2}T}}{\frac{p_{O2}V}{R_{O2}T} + \frac{p_{inert}V}{R_{inert}T}}\dot{m}_{tot} =$$

$$\frac{p_{O2}R_{inert}}{p_{O2}R_{inert} + p_{inert}R_{O2}}\dot{m}_{tot} \quad (3.10)$$

Applying Eq. 3.10 to $W_{eng,in}$ gives.

$$W_{eng,in,O2} = \frac{p_{im,O2}R_{inert}}{p_{im,O2}R_{inert} + p_{im,inert}R_{O2}}W_{eng,in,tot} \quad (3.11)$$

$$W_{eng,in,inert} = \frac{p_{im,inert}R_{O2}}{p_{im,O2}R_{inert} + p_{im,inert}R_{O2}}W_{eng,in,tot} \quad (3.12)$$

To get the fuel flow in kg/second instead of kg/stroke Eq. 3.13 is used.

$$W_{fuel} = \frac{\delta N_{eng} N_{cyl}}{120} \quad (3.13)$$

During the combustion, the oxygen is burned in the presence of fuel. The oxygen that goes out of the engine in the unburned oxygen, Eq. 3.14.

$$W_{eng,out,O2} = max\left(W_{eng,in,O2} - W_{fuel}\left(\frac{O}{F}\right)_s, 0\right) \tag{3.14}$$

The mass of the inert gas that goes out of the engine is the mass of the inert gas that goes in to the engine plus the fuel mass and the burned mass of the oxygen, 3.15.

$$W_{eng,out,inert} = W_{eng,in,inert} + W_{fuel} + min\left(W_{fuel}\left(\frac{O}{F}\right)_s, W_{eng,in,O2}\right) \tag{3.15}$$

The max and min functions are needed incase the engine will be run on fuel surplus to avoid negative oxygen flow and an inert mass flow larger than the total flow into the engine.

Eq. 3.16 shows how the exhaust temperature is modeled.

$$T_{em} = T_{im} + \frac{Q_{LHV} f_{T_{em}}\left(W_{fuel} N_{eng}\right)}{c_{p,exh}\left(W_{eng,in} + W_{fuel}\right)} \tag{3.16}$$

3.3.4 Exhaust Manifold

The pressure in the exhaust manifold, p_{em}, is modeled in the same way as the intake manifold pressure.

$$\dot{p}_{em,O2} = \frac{R_{O2} T_{em}}{V_{em}}\left(W_{eng,out,O2} - W_{egr,O2} - W_{trb,O2}\right) \tag{3.17}$$

$$\dot{p}_{em,inert} = \frac{R_{inert} T_{em}}{V_{em}}\left(W_{eng,out,inert} - W_{egr,inert} - W_{trb,inert}\right) \tag{3.18}$$

where

$$p_{em,tot} = p_{em,inert} + p_{em,O2} \tag{3.19}$$

3.3.5 EGR

The total EGR flow is modeled as a compressible isentropic flow through a restriction [1], Eq. 3.20.

$$W_{egr,tot} = A_{egr}\frac{p_{em}}{\sqrt{T_{em} R}}\Psi\left(\frac{p_{im}}{p_{em}}, \gamma_e\right) \tag{3.20}$$

where

$$\Psi\left(\frac{p_{im}}{p_{em}}, \gamma_e\right) =$$

$$\begin{cases} \sqrt{\frac{2\gamma_e}{\gamma_e-1}\left(\left(\frac{p_{im}}{p_{em}}\right)^{\frac{2}{\gamma_e}} - \left(\frac{p_{im}}{p_{em}}^{\frac{\gamma_e+1}{\gamma_e}}\right)\right)} & \text{if } \frac{p_{im}}{p_{em}} \geq \left(\frac{2}{\gamma_e+1}\right)^{\frac{\gamma_e}{\gamma_e-1}} \\ \sqrt{\gamma_e\left(\frac{2}{\gamma_e+1}\right)^{\frac{\gamma_e+1}{\gamma_e-1}}} & \text{else} \end{cases} \tag{3.21}$$

In this model the velocity of the gas cannot be greater than the speed of sound. The pressure ratio when this happens is defined by Eq. 3.22.

$$\frac{p_{im}}{p_{em}} = \left(\frac{2}{\gamma_e+1}\right)^{\frac{\gamma_e}{\gamma_e-1}} \tag{3.22}$$

The active area function A_{egr} is a map calibrated from measurement data, Eq. 3.23.

$$A_{egr} = f(u_{egr}) \tag{3.23}$$

The division of the flow into two parts is made as described earlier.

$$W_{egr,O2} = \frac{p_{em,O2}R_{inert}}{p_{em,O2}R_{inert} + p_{em,inert}R_{O2}} W_{egr,tot} \tag{3.24}$$

$$W_{egr,inert} = \frac{p_{em,inert}R_{O2}}{p_{em,O2}R_{inert} + p_{em,inert}R_{O2}} W_{egr,tot} \tag{3.25}$$

3.3.6 Turbine

The total flow through the turbine is modeled from a map, Eq. 3.26 that depends on the speed of the turbine, the position of the VGT and the pressure ratio between p_{em} and p_{es}.

$$W_{trb,tot} = f_{W_{trb}}\left(\frac{p_{em}}{p_{es}}, n_{trb}, u_{vgt}\right) \tag{3.26}$$

Also here the flow is divided as described earlier.

$$W_{trb,O2} = \frac{p_{em,O2}R_{inert}}{p_{em,O2}R_{inert} + p_{em,inert}R_{O2}} W_{trb,tot} \tag{3.27}$$

$$W_{trb,inert} = \frac{p_{em,inert}R_{O2}}{p_{em,O2}R_{inert} + p_{em,inert}R_{O2}} W_{trb,tot} \tag{3.28}$$

3.3.7 Exhaust System

The difference between the exhaust system and the other control volumes is that it is represented with only one state. One state is enough because the composition of this gas is not interesting since it can not be recirculated. In Eq. 3.29 R_{exh} is a constant for the total exhaust gas flow.

$$\dot{p}_{es} = \frac{R_{exh}T_{em}}{V_{es}}\left(W_{trb,O2} + W_{trb,inert} - W_{es}\right) \tag{3.29}$$

The flow out of the exhaust system is modeled with a quadratic restriction as in Eq. 3.30.

$$W_{es}^2 = \frac{p_{es}}{k_{es} R_{exh} T_{es}} \left(p_{es} - p_{amb}\right) \tag{3.30}$$

where k_{es} is calculated from measurement data.

3.3.8 Turbocharger

The turbocharger consists of a turbine shaft, a turbine and a compressor that inflicts torque on the shaft. The dynamics in the turbine shaft come from the build up of moment of inertia. The mass is accelerated by the torque difference of the turbine and the compressor.

$$\omega_{trb} = \frac{1}{J_{trb}} \left(\tau_{trb} - \tau_{cmp}\right) \tag{3.31}$$

The torque from the turbine is modeled from Eq. 3.32

$$\tau_{trb} = \frac{W_{trb} c_{p_{exh}} T_{em} \eta_{trb}}{\omega_{trb}} \left(1 - \left(\frac{p_{em}}{p_{es}}\right)^{\frac{1-\gamma_{exh}}{\gamma_{exh}}}\right) \tag{3.32}$$

where the efficiency, η_{trb}, is mapped from measurement data.

$$\eta_{trb} = f_{\eta_{trb}} \left(\frac{p_{em}}{p_{es}}, n_{trb}, u_{vgt}\right) \tag{3.33}$$

The torque from the compressor is modeled from Eq. 3.34

$$\tau_{cmp} = \frac{W_{cmp} c_{p_{air}} T_{amb}}{\eta_{cmp} \omega_{cmp}} \left(\left(\frac{p_{im}}{p_{amb}}\right)^{\frac{\gamma_{air}-1}{\gamma_{air}}} - 1\right) \tag{3.34}$$

where the efficiency, η_{cmp}, is mapped from measurement data.

$$\eta_{cmp} = f_{\eta_{cmp}} \left(\frac{p_{im}}{p_{amb}}, n_{trb}\right) \tag{3.35}$$

Chapter 4

Observer design

4.1 Properties of the Observed System

Before starting designing the observer the properties of the system from chapter 3 will be analyzed. Two things that has to be clarified are if the system is stable and if it is observable. Observability is needed for the observer to be able to estimate the states from the measured signals. In this analysis the system has been linearized in stationary operating points covering the whole working area of the engine. After linearizing, linear control theory has been applied to the system to understand the behavior. The assumption is made that if stability and observability can be proven for all linearizations, the non linear system will be stable and observable in the working area.

What concerns the stability, the system is stable in all the linearizations. Figure 4.1 shows an example of a pole placement at 1300 rpm and δ=150mg/stroke. The pole diagram looks similar for all stationary operating points, with one fast pole somewhere between -1500 and -100. This fast pole comes from the $p_{im,O2}$ state. The combination of one fast pole and several slow ones gives the system stiff characteristics. This can cause problem when solving the systems differential equations and the linearized model's A-matrix is ill conditioned. The A-matrix causes problems later in this chapter.

To analyze the observability of the system the observability matrix is calculated as Eq. 4.1. If the rank of this matrix is full, the system is observable.

$$\begin{bmatrix} C \\ CA \\ \vdots \\ CA^{n-1} \end{bmatrix} \tag{4.1}$$

Computing this matrix for the linearizations does not give full rank, so this method cannot prove that the system is observable. However there is reason to believe that the fact that the observability matrix does not have full rank

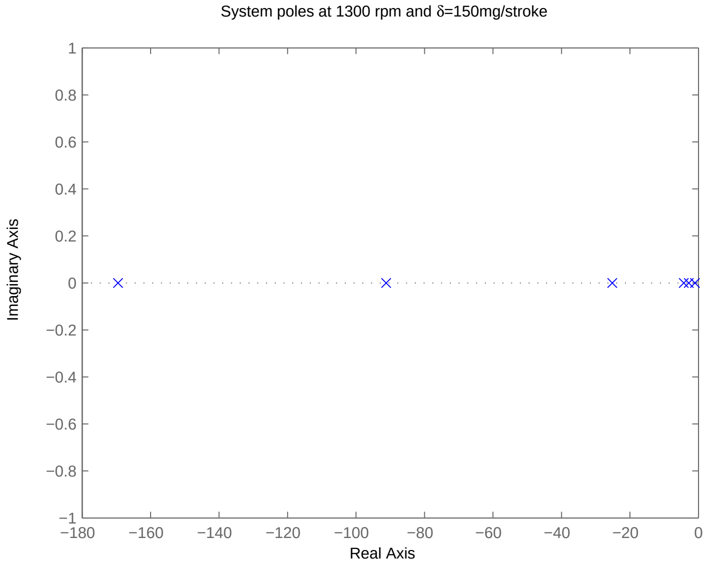

Figure 4.1: Example of pole placement

is due to numerical errors when computing it, caused by the stiffness of the system that makes it hard to calculate multiple matrix powers.

To further investigate the observability, another method has to be used. According to [3] the system is observable if the matrix in Eq. 4.2 has rank n^2, in this case 36. This matrix is larger than Eq. 4.1 but it doesn't include any matrix powers that can cause numerical problems. There was less computational problems with the second method, and the rank of the matrix was 36 for all linearizations, but this method might also become problematic if the model is expanded with more states.

$$\begin{bmatrix} I_n & 0 & \dots & 0 & 0 & 0 & \dots & 0 & 0 & C^t \\ -A^t & I_n & \dots & 0 & 0 & 0 & \dots & 0 & C^t & 0 \\ 0 & -A^t & \dots & 0 & 0 & 0 & \dots & C^t & 0 & 0 \\ \vdots & \vdots & & \vdots & \vdots & \vdots & & \vdots & \vdots & \vdots \\ 0 & 0 & \dots & I_n & 0 & C^t & \dots & 0 & 0 & 0 \\ 0 & 0 & \dots & -A^t & C^t & 0 & \dots & 0 & 0 & 0 \end{bmatrix} \tag{4.2}$$

With the system stable and observable for all linearizations, the system is considered stable and observable in the working area.

4.2 Design Method

In this thesis a simplified kind of Extended Kalman Filtering, EKF, has been used when designing the observer. EKF is an extension of the ordinary Kalman observer, that can be used on non linear systems. When using EKF the observed system is described as in Eq. 4.3 and Eq. 4.4.

$$\dot{x} = f(x, u) + w; w \sim N(0, Q) \tag{4.3}$$

$$y = h(x, u) + v; v \sim N(0, R) \tag{4.4}$$

where w is the process noise, i.e. the difference between the model and the real system, and v is the measurement noise. The intensity of the noise is described by the intensity matrices R and Q. In the model from chapter 3 the states x, the input signals u and the measured signals are defined as follows:

$$x = [p_{im,O2}, p_{im,inert}, p_{em,O2}, p_{em,inert}, p_{es}, n_{trb}]^t$$

$$u = [N_{eng}, \delta, T_{im}, p_{amb}, T_{amb}, u_{egr}, u_{vgt}]^t$$

$$y = [p_{im}, p_{em}, n_{trb}]^t$$

Having described the model as in Eq. 4.3 and Eq. 4.4 an observer can be designed as Eq. 4.5 [2].

$$\dot{\hat{x}} = f(\hat{x}, u) + K\,(y - h(\hat{x}, u)) \tag{4.5}$$

Using EKF, the gain K is continuously calculated from Eq. 4.6 and Eq. 4.7.

$$\dot{P} = F(\hat{x}, u)P + PF^t(\hat{x}, u) + Q - PH^t(\hat{x}, u)R^{-1}H(\hat{x}, u)P \tag{4.6}$$

$$K = PH^t(\hat{x}, u)R^{-1} \tag{4.7}$$

where $F(\hat{x}, u)$ and $H(\hat{x}, u)$ are linearizations of f and h respectively and P is the variation of the estimation error.

In the original extended Kalman theory, the model is supposed to be linearized around the current estimated operating point in every time step. This operation uses too much computing power to be feasable in this application, and is therefore not considered. To reduce the needed computing power, the linearizations of f are made off-line for different inputs covering the engines working area. h is a linear constant so it is not needed to be linearized. This simplified EKF observer switches between the linerarization of f, and uses the linearization closest to the current input. The model was linearized for the following different inputs:

$$T_{im} = 305K$$

$$N_{eng} = [500, 1000, 1100, \ldots, 1900, 2000]rpm$$

$$\delta = [0, 50, \ldots, 250]ml/stroke$$

$$u_{vgt} = [30, 40, 50, 60, 70, 90]$$

$$u_{egr} = [0, 5, 10, 20, 40, 60, 90]$$

$$T_{amb} = 298K$$

$$p_{amb} = 99000Pa$$

12 engine speeds, 6 fuel loads, 6 VGT positions and 7 EGR positions gives 3024 different linearizations of the model. All linearizations corresponds to stationary operating points.

4.3 Calculating Noise Matrices

In this thesis Q and R are assumed to be diagonal matrices, with one scalar noise component for every state and measured signal, as in Eq. 4.8 and 4.9. This assumption is made to reduce the complexity of the problem.

$$Q = \begin{bmatrix} Q_1 & 0 & 0 & 0 & 0 & 0 \\ 0 & Q_2 & 0 & 0 & 0 & 0 \\ 0 & 0 & Q_3 & 0 & 0 & 0 \\ 0 & 0 & 0 & Q_4 & 0 & 0 \\ 0 & 0 & 0 & 0 & Q_5 & 0 \\ 0 & 0 & 0 & 0 & 0 & Q_6 \end{bmatrix} \tag{4.8}$$

$$R = \begin{bmatrix} R_1 & 0 & 0 \\ 0 & R_2 & 0 \\ 0 & 0 & R_3 \end{bmatrix} \tag{4.9}$$

The measured data that is used comes from an European Transient Cycle, ETC. An ETC is a standardized cycle that runs the engine on different loads and engine speeds. The measured signals are sampled at 100 Hz and Figure 4.2 shows the frequency content for the intake manifold pressure. The peaks in the frequency content are dependent on the engine speed, and probably derives from the turbulence caused by the opening and closing of the cylinder valves. Since the model is a mean value model that does not take the cylinder movement into consideration, this can be considered as noise. Modeling the frequency content of the noise of the measured signal is beyond the scope of this thesis, so the noise is assumed to be white for simplicity.

Some interesting things concerning the magnitude of the noise can be noticed in Figure 4.3. One is that the n_{trb} signals is zero the first ten seconds of the plot. This is because the sensor measuring the turbine speed does not respond to speeds lower than 20000 rpm. This can be interpreted as if the measurement noise for the turbine shaft is infinite when $n_{trb} \leq 20000$. Another interesting thing to notice is that the p_{im} signals is more noisy at high pressures. Since the pressure is high when the turbine speed is high, the turbine speed seems to be a important factor for the noise magnitude.

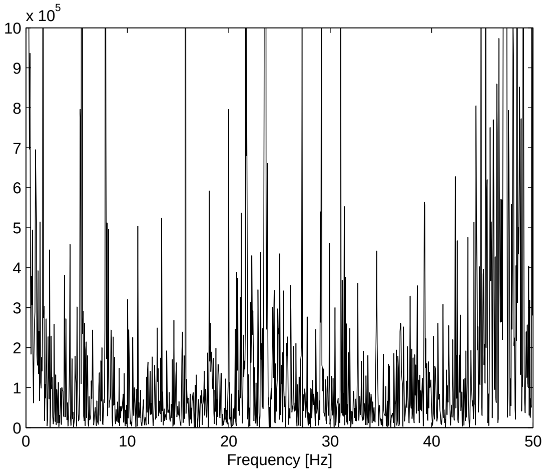

Figure 4.2: Frequency content in intake manifold pressure signal

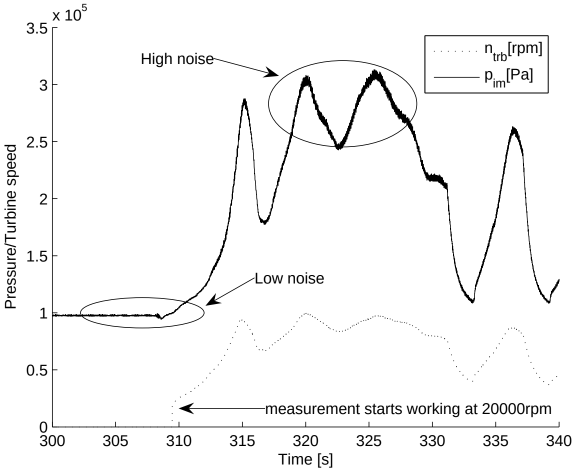

Figure 4.3: Turbine speed and intake manifold pressure

4.3.1 Calculating R

To extract the measurement noise from the measured signals, the signals are high pass filtered at 2 Hz. The remaining signal after the filtering is assumed to be measurement noise. As was mentioned earlier in this chapter, one important factor that affects the noise is the turbine speed. With similar reasoning it can be concluded that also the engine speed has a impact on the noise.

Knowing this, the measured data from all three measured signals are high pass filtered. The absolute value of the high pass filtered signal is then low pass filtered, giving an approximation of the noise intensity. To the intensity, an analytical function depending on N_{eng} and n_{trb} is calibrated using the least squares method. Eq. 4.10 shows the equation. One option could have been to map the noise, but a polynomial expression with second order terms captures the trends accurate enough and is simpler.

$$R_i = k_1 + k_2 n_{trb} + k_3 n_{trb}^2 + k_4 N_{eng} + k_5 N_{eng}^2 \tag{4.10}$$

Figure 4.4 shows the measurement noise for p_{im}. As can be seen the noise increases with the speeds. The measurement noise for n_{trb} is set to 100000 when $n_{trb} \leq 25000$ to compensate for the bad measurement in that region. 25000 is used as the threshold for the bad measurement of n_{trb} to have some safety margin if the measurement stops at a higher speed than 20000.

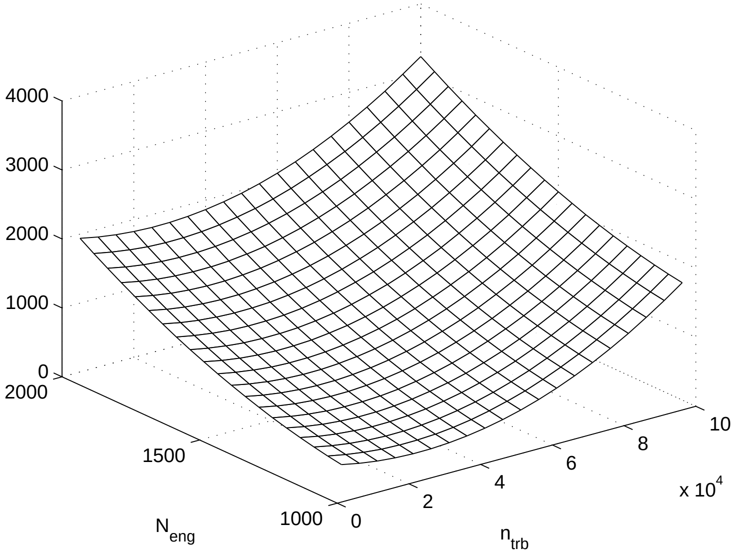

Figure 4.4: Intake manifold pressure measurement noise

4.3.2 Calculating Q

Two approaches to calculating the process noise has been examined. Method 1 approximates the noise as the difference between the modeled value of the state and the measured value. When comparing the modeled signals with the measured, the measured signals are low pass filtered with a non causal filter at 2 Hz to remove the assumed measurement noise. Eq. 4.11 shows how the noise is calculated from the difference between the model and the filtered measured signals, $\tilde{y}$.

$$w_i = h_i(\hat{x}, u) - \tilde{y}_i \tag{4.11}$$

The intensity of this noise is calculated in the same way as for the measurement noise. Since there are states for the pressure of the inert gases and the oxygen but these has not been able to measure, it is assumed that the inert part and the oxygen part will have the same noise intensity that is calculated from $p_{im,tot}$ and $p_{em,tot}$. p_{es} is assumed to have the same process noise as p_{im}, when both these pressures are easier to modulate than p_{em}. An analytical function, Eq. 4.12, has been calibrated to the model noise with the least square method in the same way as for the measurement noise.

$$Q_i = k_1 + k_2 n_{trb} + k_3 n_{trb}^2 + k_4 N_{eng} + k_5 N_{eng}^2 \tag{4.12}$$

Method 2 of calculating the process noise is more closely linked to the theoretical way of defining the noise. Here the noise is the difference between the slopes of the measured and the modeled signals. Eq. 4.13 shows how the noise is calculated. Also here $\tilde{y}$ is low pass filtered to remove noise before differentiated. This noise is represented by a function in the same way as method 1.

$$w_i = f_i(\hat{x}, u) - \dot{\tilde{y}}_i \tag{4.13}$$

Figure 4.5 and Figure 4.6 shows the two different process noises for n_{trb}. At high turbine speeds and engine speeds around 1300 to 1500 rpm the two models results in similar process noises, but method one yields almost twice as high process noise for low turbine speeds.

The fact that model one get a higher process noise when the engine speed is lower can be explained by the ETC on which the models are calibrated. The engine speed is more steady when it is around 1500 rpm than around 1000 rpm in the ETC, and the absolute error between the model and the measured value is smaller in steady state than in transients. This phenomenon doesn't affect the second method since it doesn't compare the absolute values, but the slopes.

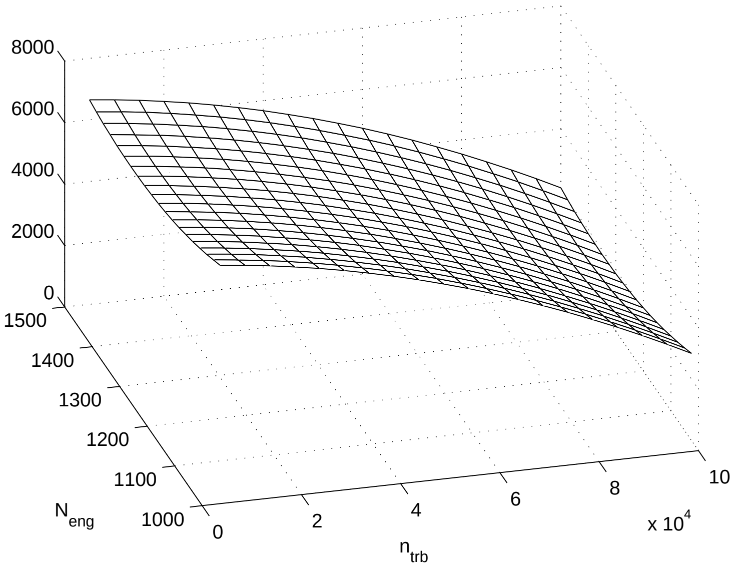

Figure 4.5: Process noise for the turbine speed with the first method

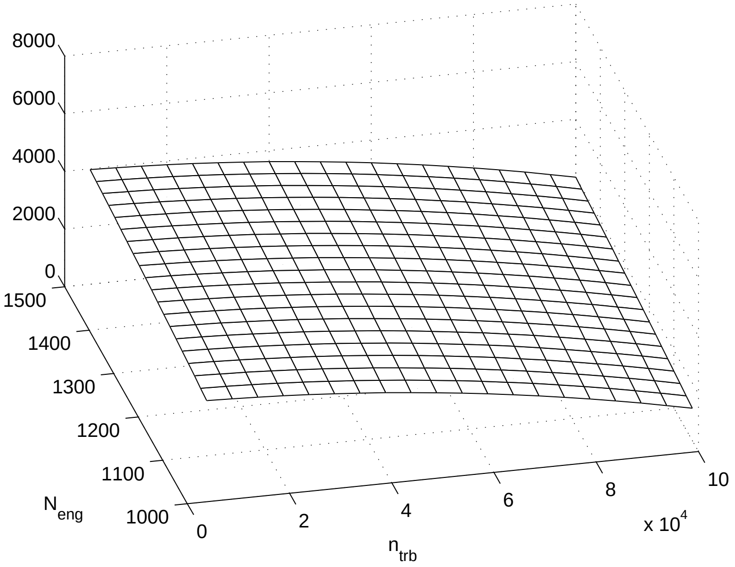

Figure 4.6: Process noise for the turbine speed with the second method

4.4 Observer designs comparisons

4.4.1 Evaluating the need for multiple linearizations

To evaluate how the number of linerarizations affect the performance of the observer, five different sets of linearizations were tested, see Table 4.1.

Table 4.1: Linearization sets

Set	N_{eng}	δ	u_{egr}	u_{vgt}	Linearizatons
1	12	6	7	6	3024
2	12	6	1	1	72
3	7	6	1	1	42
4	3	3	1	1	9
5	1	1	1	1	1

When evaluating how good the observer is with different numbers of linearizations and different ways to calculate Q, p_{im} and p_{em} are studied. All these observers estimates these pressures with the same noise level as if the signals were filtered with a 2 Hz low pass filter. With equal noise level, the performance of the observers are determined by the relative mean value error between the observed signals and non causal low pass filtered p_{im} and p_{em}. The observers were simulated with ETC data.

Table 4.2: Relative mean value error

Set	p_{im} Method 1	p_{im} Method 2	p_{em} Method 1	p_{em} Method 2
1	0.93%	1.08%	4.50%	4.07%
2	0.90%	1.05%	4.33%	3.84%
3	0.82%	1.03%	4.33%	3.82%
4	0.75%	0.81%	4.50%	4.46%
5	0.72%	0.83%	5.01%	4.16%

The results of the simulation in Table 4.2, shows that in neither of the cases tested was the largest set of linearizations the best one. In fact method one estimated p_{im} the best with only one linearization. To estimate p_{em} set 3 was the best choice for both methods of deciding Q, with the smallest error.

One reason why method 1 is better at estimating p_{im} is that it yields a larger turbine model error than method 2 at low turbine speeds, as discussed in the previous section, and a well estimated turbine speed is important for the intake manifold pressure.

4.4.2 Evaluating the possibility to calculate K off-line

In [8] and [9] Andersson and Eriksson used Kalman filtering when designing an observer for a turbo charged spark ignited(SI) engine. They switched between pre calculated gains instead of calculating them continuously. This proved to be an efficient way to implement an observer for a non linear system similar to the one in this thesis. It is interesting to see how well this kind of observer can compete with the simplified EKF, since running even the simplified EKF on board a truck is hard to do with today's computing power.

To evaluate this, one linearization was used. For this single linearization different K has been calculated. The differences between the gains are that the noise matrices has been evaluated for different n_{trb}. During the simulation the observer switches between these K depending on the current n_{trb}. This simulation was repeated with 4, 10, 20 and 50 filters to see how the number of gains affect the result. Table 4.3 shows how the result of this observer varies with the number of filters used. Also in this test, the performance of the observer gets worse when the number of filters gets too large.

Table 4.3: Simulation results

Number of K	Mean value error in p_{im}
4	1.44%
10	0.87%
20	0.89%
50	0.90%

With the best set of filters, 10 filters, the relative mean value error is 0.87%, a 20% larger error than with the best simplified EKF observer. This is a small cost for making it possible to run the observer in real time on board a truck. In the evaluation in the next section the observer with only 10 filters will be used.

4.5 Evaluation

4.5.1 Comparison with low pass filtering

One of the objectives with the observer has been to observe signals and remove the noise, but still keep the good dynamics that is lost when low pass filtering. The key to be able to calculate mass flows well is to have nice pressure signals, since most mass flows are calculated from these. The evaluation of the observer shows that the intake manifold pressure can be accurately estimated when switching between only 10 gains. This observer can be implemented on board a truck and used to estimate the intake manifold pressure instead of filtering the measured signal.

Figure 4.7 show how well the estimated p_{im} signal follows the non causal filtered pressure, referred to as mean value in the picture, during a transient. To get this good behavior when using a low pass filter, the bandwidth has to be at least 10 Hz. Figure 4.8 is a close up on the noise of the signal, here the estimated pressure has almost no noise compared to the measured signal filtered at 10 Hz.

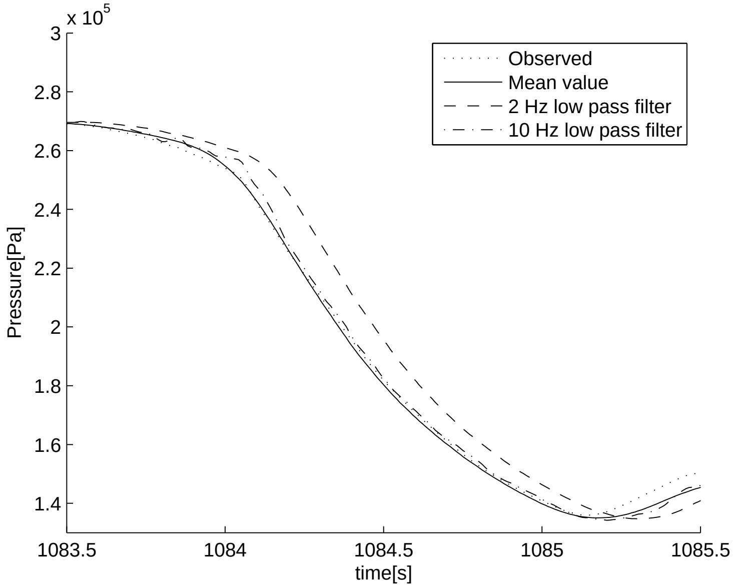

Figure 4.7: Step response in intake manifold pressure

While the observer is a good alternative to filtering for the intake manifold pressure, the exhaust manifold pressure estimation is not accurate enough to compete with a low pass filter.

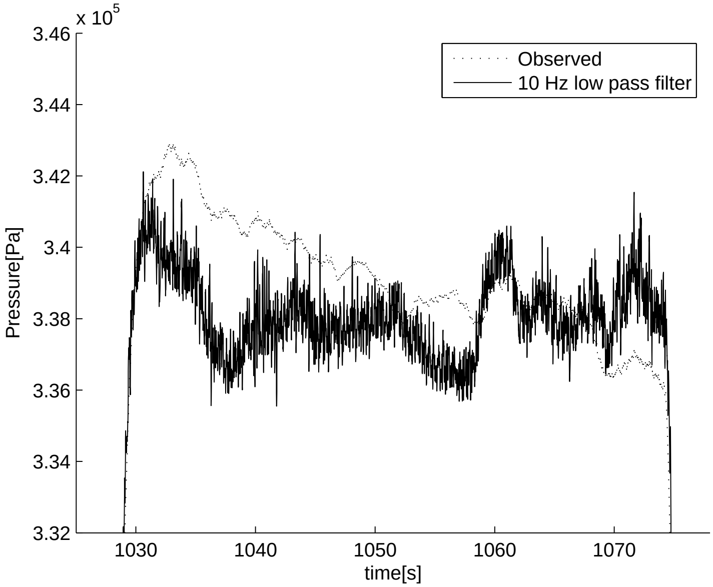

Figure 4.8: Noise comparison between filter and observer

4.5.2 Evaluation of λ observer

The main purpose with the observer was to estimate λ without using the conventional method with a mass flow sensor situated at the compressor. That method uses Eq. 4.14 to calculate the EGR flow, and then uses Eq. 2.4 to calculate λ. The last term in Eq. 4.14 compensates for the pressure build up in the intercooler.

$$W_{egr} = W_{eng,in} - \left(W_{sensor} - \frac{\dot{p}_{im} V_{int}}{R_{air} T_{im}} \right) \tag{4.14}$$

A draw back with the conventional method is that it uses the differentiation of p_{im}, which is a noisy signal. Another one is that the mass flow sensor itself has low frequency noise that is impossible to filter without loosing too much of the dynamic properties of the signal.

In Figure 4.9 the old way of calculating λ is compared with the observed λ. The figure shows 100 seconds from an ETC. The λ-signal calculated from the sensor has been filtered with a 5 Hz non causal low pass filter to make it easier to view, but still the appearance of the observed signal is much better. Unfortunately there is an offset error between the observed λ and the conventional λ, and this derives from the different methods of calculating the EGR flow. The offset can be removed with calibration, but there will still be some cases where the these flows are different. A way of removing the uncertainty

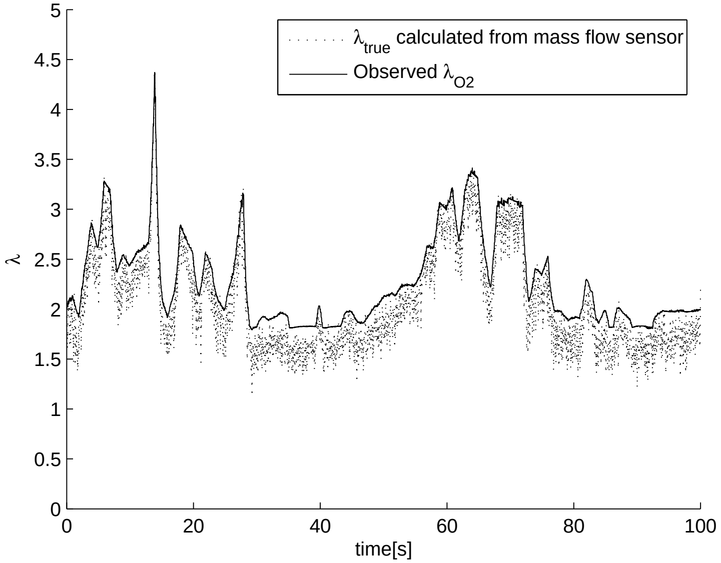

Figure 4.9: Lambda calculation comparison

in the EGR flow model is to let the observer use the mass flow sensor and calculate the flow from the old model. However this is not possible to do with the present observer feedback. The change of EGR flow model makes the observer unstable.

Since the observer models an oxygen concentration build up in transients from the exhaust manifold to the intake manifold, the λ-signal is low pass filtrated. This low pass filtration reduces the need for a very accurate EGR flow model and makes the observed oxygen concentration in the intake manifold robust against a EGR flow model error. If this robustness is enough to use the observed λ for controlling the engine has to be tested further.

Chapter 5

Validation of EGR flow

5.1 Introduction

The observed quantity that would be the most interesting to validate in this thesis is the oxygen concentration in the intake manifold, since this is the main purpose of the observer. Unfortunately the low temperature in the intake manifold made it impossible to get a concentration sensor to work there. Instead focus was put on validating the EGR flow model during transients since this is the most uncertain part of the model. The EGR flow model has only been validated in steady state earlier. The reason why the dynamics of the EGR flow model has not been validated is that the conventional method for measuring EGR flow is designed for accurate measurement in steady state only. Putting a mass flow sensor in the EGR system is not possible. The temperature is too high and mass flow sensors do not work when the gas is not clean. Instead a more innovative method was examined. The idea with this method is to put a catalytic converter in the EGR system and measure the pressure drop over it. From this pressure drop the flow can be calculated.

5.2 The Catalytic Converter Experiment

5.2.1 Theoretical Background

The idea of using a catalytic converter to produce a pressure drop was proposed by [4]. The particularity with using a catalytic converter instead of a squared restriction is that in the case with the catalytic converter, the pressure drop will have a linear relation with the mass flow for certain mass flows. This phenomenon is due to the fact that the converter consists of multiple pipes that reduces the turbulence of the gas. Reducing the turbulence is an important issue in the EGR system, since it is a very turbulent environment.

and the more turbulence there is, the more unreliable the measured differential pressure will be.

5.2.2 Experimental Setup

In this experiment a custom made catalytic converter replaced the pipe between the exhaust manifold and the EGR valve. The catalytic converter is 30 cm with a 2 cm long catalytic substrate in the middle. The shape of the pipe before and after the substrate is designed to reduce turbulence. The pressure is measured in both ends of the pipe by two 10 bar Kistler sensors. 50 cm pipes connected the sensors with the points of measurement to protect the sensors from excessive heat.

To understand the behavior of the catalytic converter in an ideal situation, the pressure drop was measured for different mass flows in a test rig and compared with the rig measurement. Figure 5.1 shows the result of the test. The mass flow is linear with the pressure drop in a non turbulent environment.

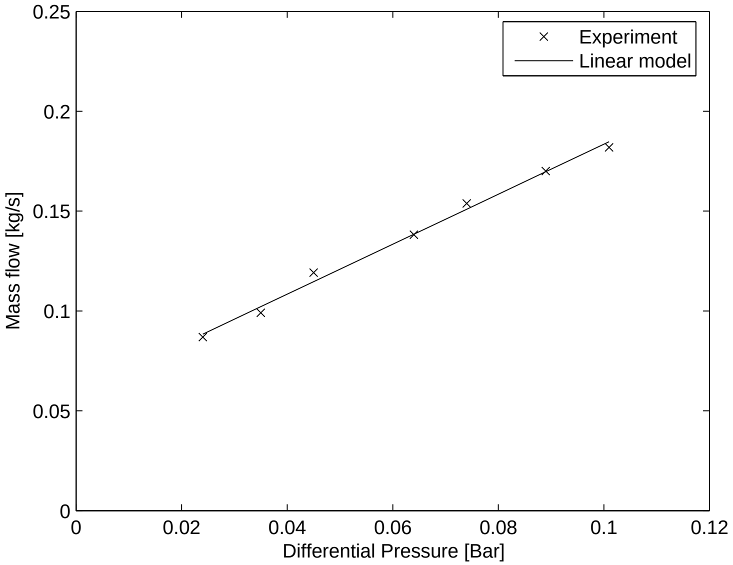

Figure 5.1: Pressure drop in experimental rig

5.2.3 Results

The engine measurements were divided into two parts. One static part that can be used for calibrating the catalytic converter model, and one European Transient Cycle(ETC) on which the observer can be evaluated. In the static part, the flow and the pressure drop was measured with different EGR valve openings and VGT positions. Different EGR and VGT positions was used to get different pressure drops. The same measurement cycle was repeated for three engine speeds, 1200 rpm, 1500 rpm and 1900 rpm.

The results were good for the measurement at 1900 rpm, where the pressure drop is linear with the EGR flow, see Figure 5.2. However as the engine speed goes down, the link between pressure drop and EGR flow becomes weaker. At 1200 rpm, Figure 5.3, the pressure drop signal is noisy even after low pass filtration at 0.5 Hz. The dynamic behavior of the pressure drop signal is also wrong. At 500 seconds in the figure, there are spikes in the pressure drop that cannot be explained by the EGR flow. Because of the problems at low engine speed, the catalytic converter test cannot be considered reliable enough to validate the performance of the EGR flow model.

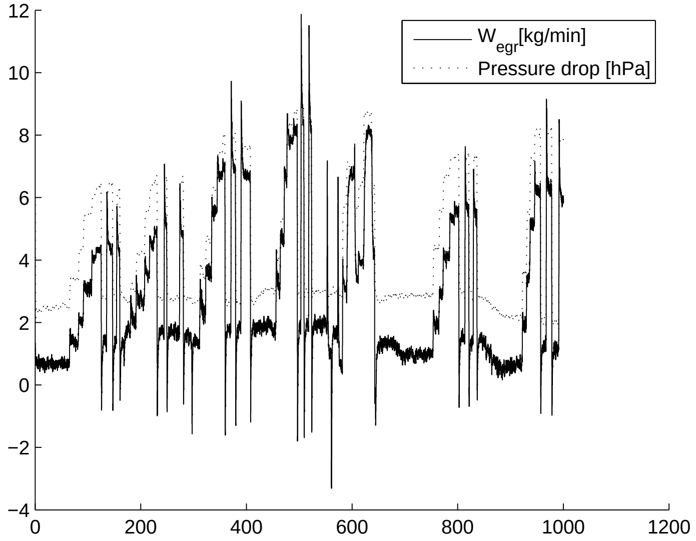

Figure 5.2: EGR flow and pressure drop at 1900 rpm

5.3 Conclusion

The fine performance at high engine speed shows that this way of measuring mass flow in a turbulent environment has the possibility to work well. If this good performance can be achieved also at lower engine speeds this can be a good measure the EGR flow in transients. To improve this measurement

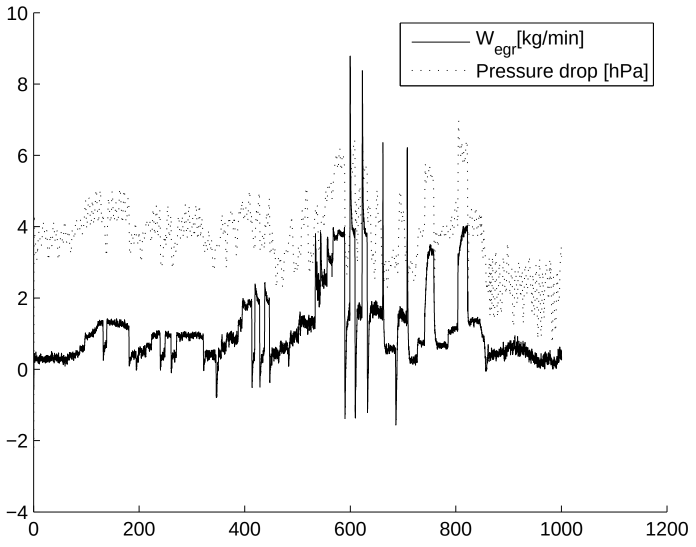

Figure 5.3: EGR flow and pressure drop at 1200 rpm

method the catalytic substrate can be made longer to further reduce the turbulence. Measuring the temperature in the converter could also be interesting.

Chapter 6

Conclusions and Future Work

6.1 Conclusions

A new engine gas flow model has been developed. This model divides the gas into one part for oxygen and one part for inert gases. Based on this model, an observer has been designed to observe the oxygen concentration in the gas. The observer can also be used to estimate the measured pressures in the intake manifold and the exhaust manifold. The advantage of estimating measurable signals with an observer instead of using a low pass filter, is that the observer uses the knowledge about the system to preserve the good dynamics of a signal while reducing the noise. What concerns the pressure in the intake manifold the observer in this thesis estimates this signal with the same noise level as a 2 Hz low pass filtered signal without considerable time delay. The observer can therefore with advantage replace a low pass filter. This is not true for the exhaust manifold pressure estimation, where the model error is too big to compete with a normal filter.

A critical issue with the observer is the uncertainty in the model of the EGR flow. It has not been possible to validate the EGR model during transient behavior. Apart from the uncertainties with the EGR flow, λ calculated with the observer have very good properties. The fact that λ_{O2}, as defined in this thesis, doesn't use the ERG flow explicitly gives a more stable signal than the conventional one. This signal is suitable for engine control purposes.

6.2 Future work

There is still interesting work that can be done in this area. Above all, measurement data from real trucks is needed to see how well λ_{O2} can be used to control the engine. The measurements in this thesis doesn't give enough understanding and support to know how good the new way of calculating λ is in a real life situation.

The observer in this thesis has been designed to estimate λ without using the mass flow sensor after the compressor. But if the sensor is not removed, it can be used to further improve the observer and make it more robust. The model can be enlarged with a control volume for the intercooler and the mass flow sensor can be integrated in the observer.

Another way to improve the observer would be to improve the EGR flow model used in the thesis. To validate this improvement it would be interesting to develop the catalytic converter test. Designing the pipe in a way to further reduce the turbulence is one enhancement. Measuring the temperature in the pipe with fast temperature sensors would also improve the understanding. The most interesting measurement though would be to measure the oxygen concentration in the intake manifold straight away. An accurate measurement of this is necessary to be able to precisely validate the need for λ_{O2} in favor of λ_{true} in transients.

Also a lot of work can still be done in trying to optimize the estimation of the measurement and process noise. In this thesis this noise has been considered as white noise, but it would be interesting to understand more about the nature of this noise.

References

[1] J. B. Heywood *Internal Combustion Engine Fundamentals*. McGrae-hill, 1988

[2] A. Gelb, J. F. Kasper Jr, R. A. Nash Jr, C. F. Price, A. A. sutherland Jr. *Applied Optimal Estimation*. Massachusetts Institute of Technology, 1974

[3] H.H. Rosenbrock State-space and multivariable theory

[4] F. Ekström and B. Andersson. Pressure Drop of Monolithic Catalytic Converters, Experimnets and Modeling. SAE 2002 World Congress, Detrit, Michigan, March 2002

[5] D. Elfvik. Modelling of a diesel engine with VGT for control design simulations. Master's thesis IR-RT-EX-0216, Department of Signals, Sensors and Systems, Royal Institute of Technology, Stockholm, Sweden, July 2002

[6] J. Ritzén Modelling and fixed step simulation of a turbo charged diesel engine. Master's thesis LiTH-ISY-EX-3442, Department of Electrical Engineering, Linköping University, Linköping, Sweden, June 2003

[7] C. Ericson Mean value modelling of a poppet valve EGR-system. Master's thesis LiTH-ISY-EX-3543, Department of Electrical Engineering, Linköping University, Linköping, Sweden, June 2004

[8] P. Andersson and L. Eriksson Obesrver based feedforward air-fuel control of turbocharged SI-engines Vehicular Systems, ISY, Linköping University, Linköping, Sweden

[9] P. Andersson and L. Eriksson Mean-value observer for a turbocharged SI-engine Vehicular Systems, ISY, Linköping University, Linköping, Sweden

Notation

Table 6.1: Symbols used in the report

Symbol	Value	Description	Unit
λ	Var	Air/fuel ratio	$-$
$EGR\%$	Var	Exhaust gas fraction	$-$
$\dot{m}$	Var	Mass flow	kg/s
W	Var	Mass flow	kg/s
N	Var	Rotational speed	rpm
n	Var	Rotational speed	rpm
ω	Var	Rotational speed	$1/s$
δ	Var	Injected fuel	$kg/stroke$
T	Var	Temperature	K
p	Var	Pressure	Pa
c_p	Con	Specific heat capacity at constant pressure	$J/(kgK)$
c_v	Con	Specific heat capacity at constant volume	$J/(kgK)$
γ	Con	Heat capacity ratio, c_p/c_v	$-$
$\tilde{R}$	Con	Universal gas constant	$10^3 J/(molK)$
M	Con	Molecular weight	kg/mol
R	Con	Gas specific constant, $\tilde{R}/M$	$J/(kgK)$
V	Con	Volume	m^3
N_{cyl}	Con	Number of cylinders	$-$
η	Var	Efficiency	$-$
η_{vol}	Var	Volumetric efficiency	$-$
Q_{LHV}	Con	Heating value	J/kg
J	Con	Moment of inertia	Nms
v	Var	Model noise	$-$
w	Var	Measurement noise	$-$
K	Var	Kalman filter	$-$
$\hat{x}$	Var	State estimation	$-$

Table 6.2: Indices used in the report

Index	Description
im	Intake manifold
em	Exhaust manifold
es	Exhaust system
d	Displacement volume per cylinder
cmp	Compressor
trb	Turbine
eng	Engine
egr	EGR system
int	Intercooler
amb	Ambient
exh	Exhaust
inert	Inert gas fraction
O2	Oxygen gas fraction
tot	All gas

Appendix A

Derivation of λ_{true}

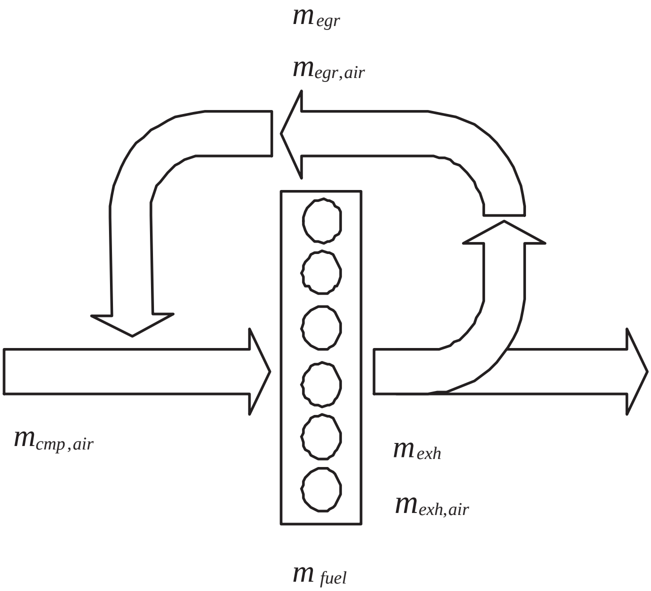

Figure A.1: Definition of mass flows

Figure A.1 and Table A.1 shows the gas flows around the engine, including EGR. In addition to the total flow, the part of the flow that consists of pure air, as defined in previous chapter, is represented as a separate flow. The gas from the compressor is always pure air, so only one flow is needed. Eq. A.1 and A.2 are basic relationships for the exhaust gas composition that are valid during steady state. In Eq. A.2 it is assumed that all the fuel will be burned

Table A.1: Description of mass flows

Name	Description
$\dot{m}_{cmp,air}$	Air flow from compressor
$\dot{m}_{egr}$	Total gas flow through EGR
$\dot{m}_{egr,air}$	Air flow through EGR
$\dot{m}_{exh}$	Total gas flow leaving cylinders
$\dot{m}_{exh,air}$	Air flow leaving cylinders
$\dot{m}_{fuel}$	Fuel mass flow

in the combustion and consume air. This is only true if λ is larger than one, however diesel engines are always run on λ larger than one, so the assumption is valid in all real scenarios.

$$\dot{m}_{exh} = \dot{m}_{cmp,air} + \dot{m}_{fuel} + \dot{m}_{egr} \tag{A.1}$$

$$\dot{m}_{exh,air} = \dot{m}_{cmp,air} + \dot{m}_{egr,air} - \left(\frac{A}{F}\right)_s \dot{m}_{fuel} = \dot{m}_{egr,air} + (\lambda_{meas} - 1)\left(\frac{A}{F}\right)_s \dot{m}_{fuel} \tag{A.2}$$

In Eq. A.3 it is assumed that the EGR flow has the same air concentration as the exhaust flow.

$$\dot{m}_{egr,air} = \dot{m}_{egr}\frac{\dot{m}_{exh,air}}{\dot{m}_{exh}} \tag{A.3}$$

Combining Eq. A.1, A.2 and A.3 gives an expression for $\dot{m}_{egr,air}$, which will be used to derive λ_{true}.

$$\dot{m}_{egr,air} = \dot{m}_{egr}\frac{\dot{m}_{exh,air}}{\dot{m}_{exh}} = \dot{m}_{egr}\frac{\dot{m}_{egr,air} + (\lambda_{meas} - 1)\left(\frac{A}{F}\right)_s \dot{m}_{fuel}}{\dot{m}_{cmp,air} + \dot{m}_{fuel} + \dot{m}_{egr}}$$

$$\Leftrightarrow \dot{m}_{egr,air}\left(1 - \frac{\dot{m}_{egr}}{\dot{m}_{cmp,air} + \dot{m}_{fuel} + \dot{m}_{egr}}\right) = \frac{(\lambda_{meas} - 1)\left(\frac{A}{F}\right)_s \dot{m}_{fuel}}{\dot{m}_{cmp,air} + \dot{m}_{fuel} + \dot{m}_{egr}}\dot{m}_{egr}$$

$$\Leftrightarrow \dot{m}_{egr,air}\left(\frac{\dot{m}_{cmp,air} + \dot{m}_{fuel}}{\dot{m}_{cmp,air} + \dot{m}_{fuel} + \dot{m}_{egr}}\right) = \frac{(\lambda_{meas} - 1)\left(\frac{A}{F}\right)_s \dot{m}_{fuel}}{\dot{m}_{cmp,air} + \dot{m}_{fuel} + \dot{m}_{egr}}\dot{m}_{egr}$$

$$\Leftrightarrow \dot{m}_{egr,air} = \frac{(\lambda_{meas} - 1)\left(\frac{A}{F}\right)_s \dot{m}_{fuel}}{\dot{m}_{cmp,air} + \dot{m}_{fuel}}\dot{m}_{egr} \tag{A.4}$$

Now that we have the expression in Eq. A.4, it is possible to find the equation for the air fuel ratio that takes both the air from the ERG and the compressor into account.

$$\lambda_{true} = \frac{\dot{m}_{cmp,air} + \dot{m}_{egr,air}}{\left(\frac{A}{F}\right)_s \dot{m}_{fuel}} = \lambda_{meas} + \frac{(\lambda_{meas} - 1)\dot{m}_{egr}}{\dot{m}_{cmp,air} + \dot{m}_{fuel}} =$$

$$= \frac{\lambda_{meas}\dot{m}_{cmp,air} + \lambda_{meas}\dot{m}_{fuel} + \lambda_{meas}\dot{m}_{egr} - \dot{m}_{egr}}{\dot{m}_{cmp,air} + \dot{m}_{fuel}} =$$

$$= \frac{\lambda_{meas}\dot{m}_{cmp,air}(1 + \frac{1}{\left(\frac{A}{F}\right)_s \lambda_{meas}}) + \dot{m}_{egr}(\lambda_{meas} - 1)}{\dot{m}_{cmp,air}(1 + \frac{1}{\left(\frac{A}{F}\right)_s \lambda_{meas}})} \tag{A.5}$$

Using the approximation in Eq. A.6, Eq. A.5 can be simplified to the expression in Eq. A.7. It can be proven that this approximation yields a relative error in λ_{true} smaller than 1%.

$$(1 + \frac{1}{\left(\frac{A}{F}\right)_s \lambda_{meas}}) = 1 \tag{A.6}$$

$$\lambda_{true} \approx \frac{\lambda_{meas}\dot{m}_{cmp,air} + \dot{m}_{egr}(\lambda_{meas} - 1)}{\dot{m}_{cmp,air}} = \frac{\lambda_{meas} - EGR\%}{1 - EGR\%} \tag{A.7}$$

LINKÖPING UNIVERSITY
ELECTRONIC PRESS

Copyright

Svenska

Detta dokument hålls tillgängligt på Internet - eller dess framtida ersättare - under en längre tid från publiceringsdatum under förutsättning att inga extraordinära omständigheter uppstår.

Tillgång till dokumentet innebär tillstånd för var och en att läsa, ladda ner, skriva ut enstaka kopior för enskilt bruk och att använda det oförändrat för ickekommersiell forskning och för undervisning. Överföring av upphovsrätten vid en senare tidpunkt kan inte upphäva detta tillstånd. All annan användning av dokumentet kräver upphovsmannens medgivande. För att garantera äktheten, säkerheten och tillgängligheten finns det lösningar av teknisk och administrativ art.

Upphovsmannens ideella rätt innefattar rätt att bli nämnd som upphovsman i den omfattning som god sed kräver vid användning av dokumentet på ovan beskrivna sätt samt skydd mot att dokumentet ändras eller presenteras i sådan form eller i sådant sammanhang som är kränkande för upphovsmannens litterära eller konstnärliga anseende eller egenart.

För ytterligare information om Linköping University Electronic Press se förlagets hemsida: `http://www.ep.liu.se/`

English

The publishers will keep this document online on the Internet - or its possible replacement - for a considerable time from the date of publication barring exceptional circumstances.

The online availability of the document implies a permanent permission for anyone to read, to download, to print out single copies for your own use and to use it unchanged for any non-commercial research and educational purpose. Subsequent transfers of copyright cannot revoke this permission. All other uses of the document are conditional on the consent of the copyright owner. The publisher has taken technical and administrative measures to assure authenticity, security and accessibility.

According to intellectual property law the author has the right to be mentioned when his/her work is accessed as described above and to be protected against infringement.

For additional information about the Linköping University Electronic Press and its procedures for publication and for assurance of document integrity, please refer to its WWW home page: `http://www.ep.liu.se/`

© Fredrik Swartling
Linköping, 15th June 2005